Haptotropic Migration from the Six- to the Five-Membered Ring of (3a,7a-Azaborindenyl)tricarbonylchromium Anion

Jun Pan, Jia Wang, Mark M. Banaszak Holl, Jeff W. Kampf, and Arthur J. Ashe, III*

Department of Chemistry, University of Michigan, Ann Arbor, Michigan 48109-1055

Received March 15, 2006

The potassium salt of (η^6-3a,7a-azaborindenyl)Cr(CO)$_3$ was prepared in a THF solution at −60 °C. Warming to −40 °C causes the Cr(CO)$_3$ group to undergo haptotropic migration to the five-membered ring. DFT calculations suggest that the preferred intramolecular pathway involves Cr(CO)$_3$ coordination to the boron rather than the nitrogen side of the ligand.

Introduction

Haptotropic rearrangements in which a π-coordinated metal migrates between different rings of polycyclic arenes have been studied extensively for nearly 30 years.[1−4] Certainly the best investigated systems have been those in which a Cr(CO)$_3$ group migrates from a neutral to an anionic ring, e.g., **1** to **2** and **3** to **4**.[5,6] We have been interested in the chemistry of B−N heteroaromatic rings that are formally constructed by replacing a C−C π-bond of a homocyclic aromatic by the isoelectronic B−N π-bond.[7] In this manner 1,2-azaborolyl **5** is derived from cyclopentadienyl[8,9] and 1,2-dihydro-1,2-azaborine **6** is derived from benzene.[7,10] In general fewer haptotropic rearrangements have been reported for heteroaromatic systems in part because most heteroaromatics are rather poor π-ligands.[11] However, both **5** and **6** are excellent π-ligands, which can serve as surrogates for cyclopentadienyl[7−9,12] and benzene[13] in metal complexes. We recently reported that complex **7** undergoes a unimolecular rearrangement to give **8**.[14] This reaction appears to be closely related to that of **1** to **2**. To explore this phenomenon further, we have investigated the isomerization of the 3a,7a-azaborindenyl-Cr(CO)$_3$ complexes **9** to **10**, which is closely analogous to the isomerization of indenyl-Cr(CO)$_3$ complexes **3** to **4** (see Scheme 1).

Results and Discussion

Tricarbonyl[η^6-3a,7a-azaborindene]chromium (**12**) was prepared in 66% yield by treating 3a,7a-azaborindene (**11**)[7b,c] with Cr(CO)$_3$(CH$_3$CN)$_3$ in THF at 25 °C for 14 h. The air-stable crystalline **12** is easily purified by column chromatography on silica gel. The ^{1}H NMR spectrum of **12** in THF-d_8 is first order and can be readily assigned by inspection (see Table 1). The allylic proton signals of the noncoordinated C$_3$H$_4$BN ring are nonequivalent due to their endo/exo relationship to the Cr(CO)$_3$ group. The signals for the C$_4$H$_4$BN ring of **12** are shifted upfield in comparison to the corresponding signals for the free ligand **11**.[15] Similar coordination shifts are seen in the ^{11}B and ^{13}C NMR spectra for the signals between **11** and **12**.[15,16] Thus η^6-complexation to the six-membered ring is indicated. This was confirmed by obtaining an X-ray crystal structure of **12**, which is illustrated in Figure 1 (see Table 2 for selected bond distances).

12 can be quantitatively deprotonated by treatment with potassium bis(trimethylsilylamide) in THF at −60 °C to afford a solution of the potassium salt of η^6-3a,7a-azaborindenyl-Cr(CO)$_3$ (**9**). The ^{1}H NMR spectrum of **9** in THF-d_8 shows a first-order pattern distinct from that of **12**. The major differences are the disappearance of the signals for the two diastereotopic allylic protons of **12** and the appearance of the characteristic three-proton signals of the azaborolide ring of **9**.[7a,8,9] Quenching **9** with excess trimethylsilyl chloride affords the 3-trimethylsilyl

* To whom correspondence should be addressed. E-mail: ajashe@umich.edu.

(1) (a) Nesmeyanov, A. N.; Ustynyuk, N. A.; Makarova, L. G.; Andre, S.; Ustynyuk, Y. A.; Novikova, L. N.; Luzikov, Y. N. *J. Organomet. Chem.* **1978**, *154*, 45. (b) Ustynyuk, N. A.; Lokshin, B. V.; Oprunenko, Y. F.; Roznyatovsky, V. A.; Luzikov, Y. N.; Ustynyuk, Y. A. *J. Organomet. Chem.* **1980**, *202*, 279.

(2) (a) Kirss, R. U.; Treichel, P. M., Jr. *J. Am. Chem. Soc.* **1986**, *108*, 853. (b) Treichel, P. M., Jr.; Johnson, J. W. *Inorg. Chem.* **1977**, *16*, 749. (c) Treichel, P. M., Jr.; Fivizzani, K. P.; Haller, K. *Organometallics* **1982**, *1*, 931.

(3) Cunningham, S. D.; Öfele, K.; Willeford, B. R. *J. Am. Chem. Soc.* **1983**, *105*, 3724.

(4) For reviews see: (a) Dötz, K. H.; Wenzel, B.; Jahr, H. C. *Top. Curr. Chem.* **2004**, *248*, 63. (b) Dötz, K. H.; Jahr, H. C. *Chem. Rec.* **2004**, *4*, 61. (c) Oprunenko, Y. F. *Russ. Chem. Rev.* **2000**, *69*, 683. (d) Morris, M. J. In *Comprehensive Organometallic Chemistry II*; Abel, E. W., Stone, F. G. A., Wilkinson, G., Eds.; Pergamon Press: New York, 1995; Vol. 5, p 501. (e) Ustynyuk, N. A. *Metalloorg. Khim.* **1989**, *2*, 43.

(5) (a) Ustynyuk, N. A.; Oprunenko, Y. F.; Malyugina, S. G.; Trifonova, O. I.; Ustynyuk, Y. A. *J. Organomet. Chem.* **1984**, *270*, 185. (b) Thoma, T.; Pleshakov, V. G.; Prostakov, N. S.; Ustynyuk, Y. A.; Nesmayanov, A. N.; Ustynyuk, N. A. *J. Organomet. Chem.* **1980**, *192*, 359. (c) Trifonova, O. I.; Galiullin, R. A.; Ustynyuk, Y. A.; Ustynyuk, N. A.; Petrovsky, P. V.; Kratsov, D. N. *J. Organomet. Chem.* **1987**, *328*, 321.

(6) (a) Ceccon, A.; Gambaro, A.; Gottardi, F.; Santi, S.; Venzo, A.; Lucchini, V. *J. Organomet. Chem.* **1989**, *379*, 67. (b) Ceccon, A.; Gambaro, A.; Gottardi, F.; Santi, S.; Venzo, A. *J. Organomet. Chem.* **1991**, *412*, 85.

(7) (a) Ashe, A. J., III; Fang, X. *Org. Lett.* **2000**, *2*, 2089. (b) Ashe, A. J., III; Yang, H.; Fang, X.; Kampf, J. W. *Organometallics* **2002**, *21*, 4578. (c) Fang, X.; Yang, H.; Kampf, J. W.; Banaszak Holl, M. M.; Ashe, A. J., III. *Organometallics* **2006**, *25*, 513.

(8) (a) Schmid, G. *Comments Inorg. Chem.* **1985**, *4*, 17. (b) Schmid, G. In *Comprehensive Heterocyclic Chemistry II*; Shinkai, I., Ed.; Pergamon: Oxford, UK, 1996; Vol. 3, p 739.

(9) (a) Liu, S.-Y.; Lo, M. M.-C.; Fu, G. C. *Angew. Chem., Int. Ed.* **2002**, *41*, 174. (b) Liu, S.-Y.; Hills, I. D.; Fu, G. C. *Organometallics* **2002**, *21*, 4323.

(10) For a review see: Fritsch, A. J. *Chem. Heterocycl. Compd.* **1977**, *30*, 381.

(11) However, see: Zhu, G.; Tanski, J. M.; Churchill, D. G.; Janak, K. E.; Parkin, G. *J. Am. Chem. Soc.* **2002**, *124*, 13658.

(12) Yang, H.; Fang, X.; Kampf, J. W.; Ashe, A. J., III. *Polyhedron* **2005**, *24*, 1280.

(13) Ashe, A. J., III; Fang, X.; Fang, X.; Kampf, J. W. *Organometallics* **2001**, *20*, 5413.

(14) Pan, J.; Kampf, J. W.; Ashe, A. J., III. *Organometallics* **2006**, *25*, 197.

(15) For a similar case, see: Ashe, A. J., III; Kampf, J. W.; Kausch, C. M.; Konishi, H.; Kristen, M. O.; Kroker, J. *Organometallics* **1990**, *9*, 2944.

(16) Elschenbroich, C.; Salzer, A. *Organometallics*, 2nd ed.; VCH Publishers: Weiheim, Germany, 1991; pp 296, 307.

10.1021/om060239+ CCC: $33.50
Publication on Web 06/03/2006

Scheme 1

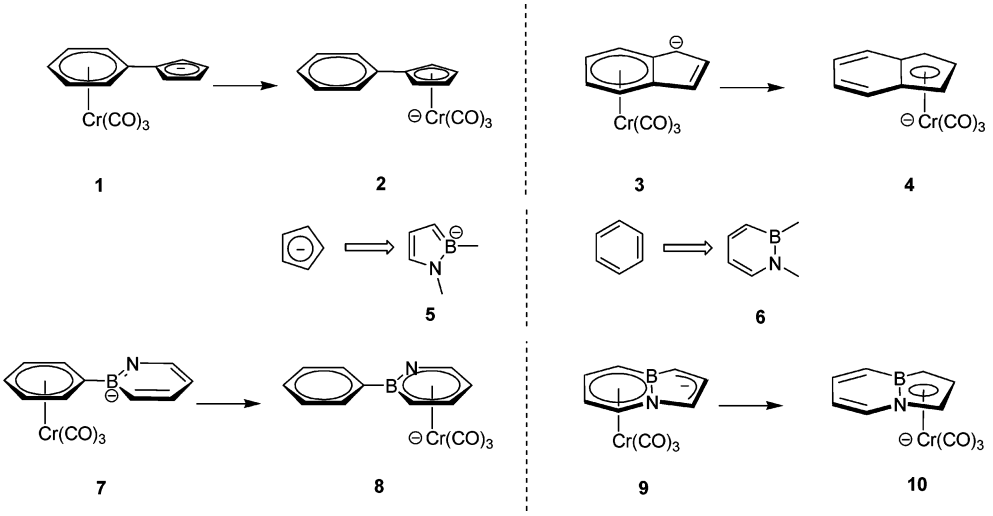

Table 1. ^{1}H, ^{13}C, and ^{11}B NMR Parameters for 9−12[a]

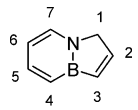

11[e]

	9[b,c]	**10**[b]	**11**[d]	**12**[b]
^{1}H				
H_1	6.49 (s)	6.39 (s)	4.38 (t, J = 1.8 Hz)	3.79, 4.28 (d, J = 19.5 Hz)
H_2	6.95 (d, J = 6.5 Hz)	4.87 (d, J = 5.3 Hz)	6.42 (br d, J = 8.0 Hz)	6.78 (d, J = 8.5 Hz)
H_3	5.96 (d, J = 6.5 Hz)	3.26 (d, J = 5.3 Hz)	6.97 (br d, J = 8.0 Hz)	6.35 (d, J = 8.5 Hz)
H_4	5.41 (d, J = 9.0 Hz)	7.14 (d, J = 11.7 Hz)	6.71 (d, J = 11.1 Hz)	4.82 (d, J = 9.5 Hz)
H_5	4.78 (dd, J = 9.0, 5.5 Hz)	6.79 (dd, J = 11.7, 6.3 Hz)	7.56 (dd, J = 11.1, 6.3 Hz)	5.86 (dd, J = 9.5, 5.5 Hz)
H_6	5.18 (t, J = 5.5 Hz)	5.79 (t, J = 6.3 Hz)	6.23 (d, J = 6.3 Hz)	5.40 (t, J = 5.5 Hz)
H_7	7.51 (d, J = 5.2 Hz)	7.01 (d, J = 6.5 Hz)	7.67 (d, J = 6.3 Hz)	7.05 (d, J = 5.0 Hz)
^{13}C				
C_1	108.0	84.2	58.8	63.4
C_2	130.4	94.0	144.2	146.8
C_3	110.3 (br)	64.9 (br)	124 (br)	131.5 (br)
C_4	95.1 (br)	135.1 (br)	133.6 (br)	82.0 (br)
C_5	90.2	131.9	142.2	108.6
C_6	82.5	111.7	109.5	81.9
C_7	100.1	131.8	135.3	103.6
^{11}B	10.6	13.6	34.2	21.8

[a] The samples were recorded on a Varian Inova-500 FT NMR spectrometer. The chemical shifts are reported in parts per million, and the coupling constants are reported in hertz. [b] The NMR spectra were recorded in THF-d_8. [c] The NMR spectra were recorded at −60 °C. [d] The ^{1}H NMR spectra were recorded in THF-d_8. The ^{11}B and ^{13}C NMR spectra were recorded in C_6D_6 (refs 7b,c). [e] The numbering scheme was chosen to be identical to that used in the X-ray structures of **12** and **15**, as shown in Figures 1 and 2.

derivative **13**, which is presumed to be exo. It had been observed that alkali metal salts of 1,2-azaborolides usually react with electrophiles at the 3-position.[17] We have previously found that 3a,7a-azaborindenylpotassium reacts with trimethylsilyl chloride to give the 3-trimethylsilyl derivative **14**.[18]

Allowing THF solutions of potassium η^6-3a,7a-azaborindenyl-$Cr(CO)_3$ (**9**) to warm to 25 °C causes it to undergo a clean isomerization to its η^5-regioisomer **10**. Alternatively **10** may be prepared by treating a THF solution of **12** with potassium bis(trimethylsilyl)amide at 25 °C. The ^{1}H NMR spectrum of **10** shows a first-order pattern that is distinct from that of **9**. Relative to **9** the ^{1}H and the ^{13}C NMR spectra of **10** show that all of the signals of the six-membered ring atoms are shifted downfield and all of the signals for the five-membered ring atoms are shifted upfield. This is consistent with a coordina-

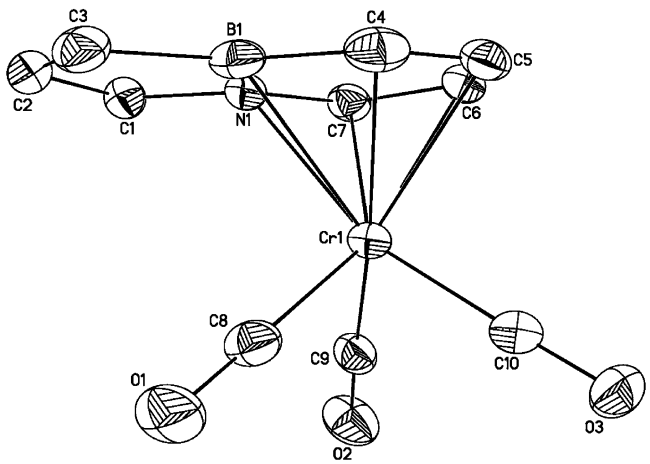

Figure 1. Solid-state structure of **12** (ORTEP). Thermal ellipsoids are at the 50% probability level. Hydrogen atoms have been omitted for clarity.

(17) (a) Schmid, G.; Zaika, D.; Lehr, J.; Augart, N.; Boese, R. *Chem. Ber.* **1988**, *121*, 1873. (b) Schmid, G.; Reschke, J.; Boese, R. *Chem. Ber.* **1994**, *127*, 1891.

(18) Ashe, A. J., III; Yang, H. Unpublished data.

Table 2. Selected Bond Lengths (Å) for 12 and 15

bond	12	15
C(1)−N(1)	1.478(2)	1.421(3)
C(1)−C(2)	1.503(2)	1.391(3)
C(2)−C(3)	1.338(2)	1.419(3)
B(1)−C(3)	1.548(2)	1.513(3)
B(1)−N(1)	1.466(2)	1.471(3)
B(1)−C(4)	1.510(2)	1.514(3)
C(4)−C(5)	1.401(2)	1.352(3)
C(5)−C(6)	1.420(2)	1.440(3)
C(6)−C(7)	1.395(2)	1.340(4)
C(7)−N(1)	1.377(2)	1.402(3)
B(1)−Cr(1)	2.362(2)	2.340(2)
C(4)−Cr(1)	2.276(1)	
C(5)−Cr(1)	2.219(1)	
C(6)−Cr(1)	2.201(1)	
C(7)−Cr(1)	2.178(1)	
N(1)−Cr(1)	2.210(1)	2.209(2)
C(1)−Cr(1)		2.145(2)
C(2)−Cr(1)		2.204(2)
C(3)−Cr(1)		2.252(2)
C(CO)-Cr(1) av	1.839(2)	1.847(4)
Sn(1)−Cr(1)		2.756(1)

tion shift of the $Cr(CO)_3$ group from the C_4H_4BN ring to the C_3H_3BN ring.[16] On the other hand the ^{11}B NMR spectra show only a very small change between **9** and **10**, as is expected since the boron atom remains coordinated to Cr in both structures.

Anion **10** may be efficiently trapped by the reaction with trimethylstannyl chloride to form adduct **15**. It had previously been observed that monocyclic (1,2-azaborolyl)$Cr(CO)_3$ anions react with tin halides to afford Cr(II) adducts analogous to **15**.[9b,19] Indeed an X-ray structure of **15** shows that the azaborolyl ring is η^5-coordinated to the Cr atom (see Figure 2 and Table 2). The isolation of **15** provides convincing independent evidence that the $Cr(CO)_3$ group has undergone a haptotropic migration from the fused azaborinyl ring of **9** to the fused azaborolyl ring of **10** (see Schemes 2, 3). It was of interest to carefully examine the haptotropic $Cr(CO)_3$ migration of **9** to **10** in order to compare it with the previously studied $Cr(CO)_3$ migration of the isoelectronic **3** to **4**. The conversion of **9** to **10** at −30 to −40 °C in THF-d_8 was easily monitored by ^1H NMR spectroscopy. No decomposition products were noted. When the reaction was performed in the presence of the good π-donors hexamethylbenzene or indenylpotassium, no cross products (<1%) were noted. These data are consistent with a unimolecular reaction. The first-order rate constants were found to be

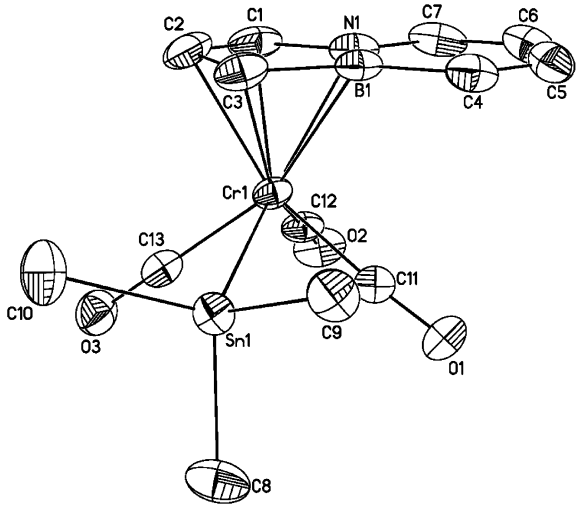

Figure 2. Solid-state structure of **15** (ORTEP). Thermal ellipsoids are at the 50% probability level. Hydrogen atoms have been omitted for clarity.

Scheme 2

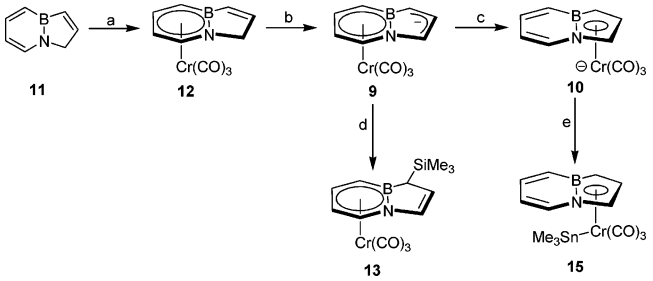

Scheme 3

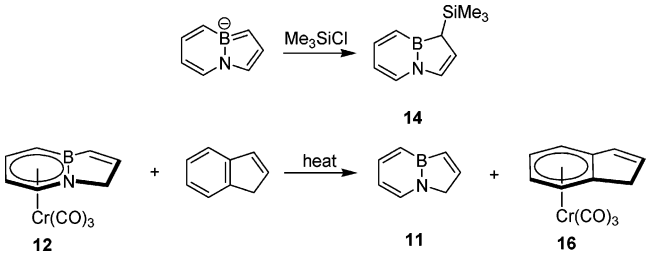

$k = 4.5 \times 10^{-5}$ s^{-1} at 233 K and $k = 13.1 \times 10^{-5}$ s^{-1} at 240 K ($\Delta G^{\ddagger} = 18.2$ kcal mol^{-1} at 240 K). For comparison the rate of conversion of **3** to **4** is nearly 100 times slower at 240 K with $k = 0.14 \times 10^{-5}$ s^{-1} ($\Delta G^{\ddagger} = 20.3$ kcal mol^{-1}).[6b]

Assuming that the two processes take place by analogous mechanisms, the faster rate is consistent with a weaker $Cr(CO)_3$ coordination to the C_4H_4BN ring of **9** than to the C_6H_4 ring of **3**. We have previously established that 1,2-azaborinyl is a weaker ligand toward $Cr(CO)_3$ than is phenyl.[14] In the present case it can be established that indene is a better ligand toward $Cr(CO)_3$ than is 3a,7a-azaborindene. Thus heating **12** in THF to 140 °C in the presence of 1 equiv of indene gives tricarbonyl-[η^6-indene]chromium (**16**) and free 3a,7a-azaborindene (**11**).

The mechanisms that have been proposed for intramolecular haptotropic migrations in carbocyclic systems such as **3** to **4** have involved stepwise π-decomplexation of the double bonds of one ring followed by or concomitant with π-complexation of the new ring.[20,21] The metal is proposed to follow a trajectory in the π-plane along the periphery of the molecule. A least motion mechanism in which the metal moves in the π-plane from the center of one ring to the center of the second ring has generally been disfavored.[20,21] It seems reasonable to assume that the mechanisms of the $Cr(CO)_3$ shifts in **9** to **10** are similar to those in **3** to **4**, with metal shifts along the molecular periphery being favored in both cases. However, the peripheral metal shift mechanism is fundamentally more complex in the heterocyclic case because of the lower symmetry. Thus the metal might shift along a path close to either the C−B−C bonds or the C−N−C bonds. We do not see an easy experimental test to choose between the two pathways.

To obtain more information about the structure of possible intermediates or transition states in the conversion of **9** to **10**,

(19) Schmid, G.; Schmidt, F.; Boese, R. *Chem. Ber.* **1985**, *118*, 1949.
(20) (a) Albright, T. A.; Hofmann, P.; Hoffmann, R.; Lillya, C. P.; Dobosh, P. A. *J. Am. Chem. Soc.* **1983**, *105*, 3396. (b) Howell, J. A. S.; Ashford, N. F.; Dixon, D. T.; Kola, J. C.; Albright, T. A.; Kang, S. K. *Organometallics* **1991**, *10*, 1852.
(21) (a) Oprunenko, Y.; Akhedov, N. G.; Laikov, D. N.; Malyugina, S. G.; Mstislavsky, V. I.; Roznyatovsky, V. A.; Ustynyuk, Y. A.; Ustynyuk, N. A. *J. Organomet. Chem.* **1999**, *583*, 136. (b) Oprunenko, Y.; Gloriozov, I.; Lyssenko, K.; Malyugina, S.; Mityuk, D.; Mstislavsky, V.; Günther, H.; von Firks, G.; Ebener, M. *J. Organomet. Chem.* **2002**, *656*, 27. (c) Dötz, K. H.; Stendel, J., Jr.; Müller, S.; Nieger, M.; Ketrat, S.; Dolg, M. *Organometallics* **2005**, *24*, 3219.

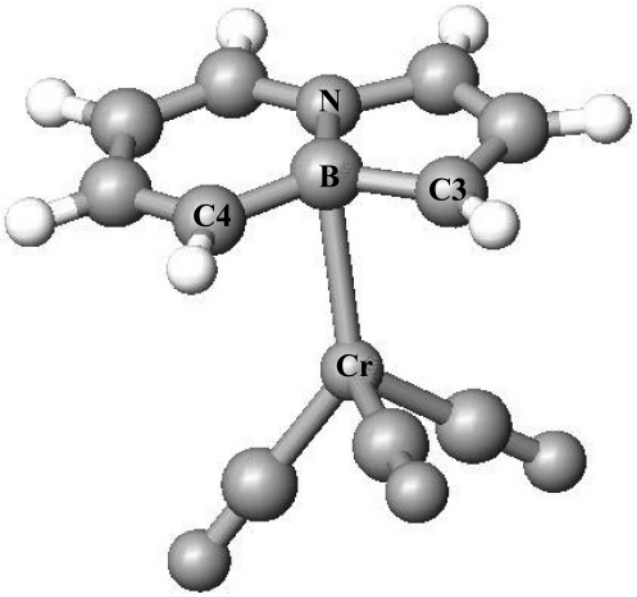

Figure 3. Calculated transition state **B**. Selected bond distances (Å): B(1)−Cr(1), 2.347; C(4)−Cr(1), 2.549; C(3)−Cr(1), 2.424; N(1)−Cr(1), 3.257.

we have performed density function theory (DFT) calculations at the B3LYP/6-31G* level. We note that DFT calculations have previously been used to identify possible transition states of haptotropic rearrangements of $Cr(CO)_3$ complexes of benzocyclic aromatics.[21] Calculations were first performed on **9** and **10**, which gave energy minima for the η^6-$Cr(CO)_3$ and the η^5-$Cr(CO)_3$ coordinated species, respectively. The isomerization was calculated to be exothermic by 12.8 kcal mol^{-1}. The calculated bond distances seem plausible when compared to the X-ray data for the analogues **12** and **15**. Tables of calculated bond distances for **9** and **10** are collected in the Supporting Information.

To economically calculate possible transition states for the $Cr(CO)_3$ migration, several restraints were placed on the system. The ring atoms were confined to a plane, but allowed to move in plane. The chromium atom was constrained to a plane containing the boron and nitrogen atoms that was perpendicular to the ring plane. Two saddle points (one imaginary vibrational frequency each) were located. In calculated transition state **B** (illustrated in Figure 3) the $Cr(CO)_3$ group sits below the boron atom.[22] Essentially the metal is π-bonded to a boron-substituted allyl group. In transition state **N** the $Cr(CO)_3$ group sits below the nitrogen atom and is π-bonded to a nitrogen-substituted allyl group.[22] Transition state **B** is 8 kcal mol^{-1} lower in energy and therefore preferred.

Since borane−metal complexes are rare,[23,24] why should transition state **B** be favored? The $Cr(CO)_3$ group is strongly electron withdrawing.[25] When the symmetrically bound $Cr(CO)_3$ group of **9** is displaced toward an unsymmetrical transition state leading to **10**, it will likely seek out the carbon atom of the five-membered ring, which has the highest negative charge density. Our DFT calculations on **9** indicate that this is the carbon atom adjacent to boron (charge at C(3) = −0.26). For comparison the carbon atom adjacent to nitrogen is indicated to be positively charged (charge at C(1) = +0.08). Tables of calculated charge densities of **9** are listed in the Supporting Information.

(22) When the restraints were relaxed, the chromium atom of **B** moved slightly toward C(3), but the chromium atom of **N** moved to give **10**.

Concluding Statements

In summary the haptotropic shift of the $Cr(CO)_3$ group that converts 3a,7a-azaborindenyl-$Cr(CO)_3$ complexes **9** to **10** seems very similar to that which converts indenyl-$Cr(CO)_3$ complexes **3** to **4**. In this respect the 3a,7a-azaborindenyl ring system is a perturbed indenyl system. However the perturbation exerted by the heteroatoms makes the ring system less symmetrical. DFT calculations indicate that the haptotropic $Cr(CO)_3$ shift favors a route along the boron rather than the nitrogen side of the molecule.

Experimental Section

General Procedures. Manipulations of air-sensitive compounds were performed under a nitrogen or argon atmosphere using standard Schlenk techniques or in a nitrogen-filled drybox. Tetrahydrofuran, pentane, and hexanes were dried and deoxygenated by distillation from sodium/benzophenone ketyl. Tetrahydrofuran-d_8 was dried over potassium/sodium alloy before using. Potassium bis(trimethylsilyl)amide (Aldrich), hexamethylbenzene (Aldrich), and indene (Aldrich) were used without further purification. ^{1}H, ^{13}C, and ^{11}B NMR spectra were recorded on a Varian Inova-500 FT NMR spectrometer at ambient temperature. Chemical shifts are reported in parts per million (δ). Proton and carbon chemical shifts are relative to respective solvent internal standards shown below: THF-d_8 δ 3.58 (^{1}H), 67.57 (^{13}C). The coupling constants (J) are reported in hertz. The following abbreviations are used to describe peak patterns: br = broad, s = singlet, d = doublet, t = triplet, q = quartet, and m = multiplet. The numbering scheme was chosen to be identical to that used in the X-ray structures of **12** and **15** as shown in Figures 1 and 2. All ^{13}C and ^{11}B NMR spectra were determined with complete proton decoupling. High-resolution mass spectra were recorded on a VG-250S spectrometer with an electron-impact at 70 eV. Elemental analyses were conducted on a Perkin-Elmer 240 CHN analyzer by the Analytical Service Department of the Chemistry Department at the University of Michigan, Ann Arbor. Melting points were determined using a MEL-TEMP apparatus (Laboratory Devices) with an uncorrected thermometer.

Tricarbonyl[3a,7a-azaborindene]chromium (12). 3a,7a-Azaborindene (**11**) (1.07 g, 9.15 mmol) in 90 mL of THF was added to $Cr(CO)_3(CH_3CN)_3$ (7.11 g, 27.43 mmol). The resulting orange suspension was stirred at room temperature for 14 h. The solvent was removed under reduced pressure. The residue was extracted with 3 × 25 mL of ethyl ether. After removal of the solvents, the crude product was purified by column chromatography on silica gel (20% ethyl acetate in hexanes elution) to yield a pure sample of the product as an orange powder (1.53 g, 66%). Recrystallization from methylene chloride/hexanes gave orange crystals, mp = 113 °C. IR (hexane film): 1980, 1916, 1896 cm^{-1}. HRMS (EI, m/z): calcd for $C_{10}H_8{}^{11}BNO_3{}^{52}Cr$ (M^+), 253.0002; found, 253.0008. Anal. Calcd for $C_{10}H_8BNO_3Cr$: C, 47.48; H, 3.19; N, 5.54. Found: C, 47.32; H, 3.26; N, 5.42.

Preparation of 9. In a sealed NMR tube, a mixture of **12** (24 mg, 95 μmol) and potassium bis(trimethylsilyl)amide (24 mg, 120 μmol) was dissolved in 0.7 mL of THF-d_8 at −60 °C. The resulting NMR showed that **9** was formed quantitatively.

Preparation of 10. In a sealed NMR tube, a mixture of **12** (24 mg, 95 μmol) and potassium bis(trimethylsilyl)amide (24 mg, 120 μmol) was dissolved in 0.7 mL of THF-d_8 at room temperature. The resulting NMR spectra showed that **10** was formed quantitatively.

(23) Braunschweig, H.; Colling, M. *Coord. Chem. Rev.* **2001**, *223*, 1.
(24) For an instructive example, see: Hill, A. F.; Owen, G. R.; White, A. J. P.; Williams, D. J. *Angew. Chem., Int. Ed.* **1999**, *38*, 2759.
(25) Nicholls, B.; Whiting, M. C. *J. Chem. Soc.* **1959**, 551.

Haptotropic Migration from 9 to 10. The haptotropic migration was carried out in sealed NMR tubes at two different temperatures and monitored by ^{1}H NMR spectroscopy. The integrals of the various proton multiplets were normalized against the signal from the hexamethylbenzene used as internal standard for the integration. Use of the first-order equation for an irreversible reaction gave satisfactory plots ($R^2 > 0.999$) up to 90% of reaction. Rate constants were determined to 1.31×10^{-4} s^{-1} at 240 K and 0.45×10^{-4} s^{-1} at 233 K. No cross product could be detected when the migration was performed in the presence of hexamethylbenzene or indenylpotassium. The migration is intramolecular.

Crossover Reaction. In a sealed NMR tube, a mixture of **12** (16 mg, 63 μmol) and indene (9 mg, 77 μmol) in 0.75 mL of THF-d_8 was heated to 140 °C for 90 min. The resulting NMR spectra showed **16** was formed as the major product. The formation of **16** was further confirmed by HRMS.

Preparation of 13. A solution of **12** (119 mg, 0.47 mmol) in 3 mL of THF was added dropwise to a solution of potassium bis(trimethylsilyl)amide (120 mg, 0.60 mmol) in 5 mL of THF at −78 °C. After the mixture was stirred at −78 °C for 30 min, a solution of Me_3SiCl (258 mg, 2.37 mmol) in 3 mL of THF was added dropwise. The resulting solution was allowed to warm to room temperature slowly and stirred overnight. The volatiles were removed under vacuum. The residue was extracted by 2 × 7 mL of CH_2Cl_2. After removal of CH_2Cl_2, the residue was washed with 2 × 6 mL of pentane at −10 °C and dried in vacuo to give the product as an orange-red powder (94 mg, 61%). Recrystallization from pentane gave red crystals, mp = 133 °C (dec). IR (hexane film): 1976, 1912, 1897 cm^{-1}. ^{1}H NMR (500 MHz, THF-d_8): δ −0.01 (s, 9H, $SiMe_3$); 2.39 (s, 1H, C(3)H); 4.91(d, J = 9.3 Hz, 1H, C(4)H); 5.36 (t, J = 5.4 Hz, 1H, C(6)H); 5.80 (dd, J = 9.3, 6.1 Hz, 1H, C(5)H); 5.99 (t, J = 3.3 Hz, 1H, C(2)H); 6.61 (d, J = 3.7 Hz, 1H, C(1)H); 7.20 (d, J = 4.7 Hz, 1H, C(7)H). ^{13}C NMR (125.7 MHz, THF-d_8): δ −1.38, 31.8 (br), 81.5, 82.2 (br), 102.1, 107.9, 128.2, 134.9, 231.7. ^{11}B NMR (160.4 MHz, THF-d_8): δ 24.2. HRMS (EI, m/z): calcd for $C_{13}H_{16}{}^{11}BNO_3Si^{52}Cr$ (M^+), 325.0398; found, 325.0404. Anal. Calcd for $C_{13}H_{16}BNO_3SiCr$: C, 48.02; H, 4.96; N, 4.31. Found: C, 47.90; H, 4.99; N, 4.25.

Preparation of 15. A solution of **12** (225 mg, 0.89 mmol) in 5 mL of THF was added dropwise to a solution of potassium bis(trimethylsilyl)amide (195 mg, 0.98 mmol) in 5 mL of THF at 0 °C. The mixture was allowed to warm to room temperature and stirred for 20 min. Then a solution of Me_3SnCl (200 mg, 1.00 mmol) in 5 mL of THF was added slowly. After stirring at room temperature for 15 min, the solvents were removed under vacuum. The residue was extracted by 3 × 10 mL of pentane, and the combined extracts were concentrated. Crystallization from a concentrated pentane solution yielded the desired product as orange crystals (298 mg, 81%), mp = 91 °C. IR (hexane film): 1981, 1915, 1889 cm^{-1}. ^{1}H NMR (500 MHz, THF-d_8): δ 0.57 (s, J(^{119}SnH) = 24 Hz, 9H, $SnMe_3$); 3.81 (d, J = 5.0 Hz, 1H, C(3)H); 4.76(d, J = 5.0 Hz, 1H, C(2)H); 6.39 (t, J = 6.5 Hz, 1H, C(6)H); 7.19 (dd, J = 11.8, 6.5 Hz, 1H, C(5)H); 7.34(m, 2H, C(4)H, C(7)H); 7.45 (s, 1H, C(1)H). ^{13}C NMR (125.7 MHz, THF-d_8): δ −2.80, 74.0 (br), 88.7, 91.7, 117.2, 131.3, 134.1 (br), 136.9. ^{11}B NMR (160.4 MHz, THF-d_8): δ 12.5. HRMS (EI, m/z): calcd for $C_{13}H_{16}{}^{11}BNO_3{}^{120}Sn^{52}Cr$ (M^+), 416.9650; found, 416.9669. Anal. Calcd for $C_{13}H_{16}BNO_3SnCr$: C, 37.55; H, 3.88; N, 3.37. Found: C, 37.72; H, 3.95; N, 3.26.

Table 3. Crystal Data and Data Collection Parameters for 12 and 15

	12	**15**
empirical formula	$C_{10}H_8BCrNO_3$	$C_{13}H_{16}BCrNO_3Sn$
fw	252.98	415.77
temp, K	123(2)	123(2)
wavelength, Å	0.71073	0.71073
cryst syst	monoclinic	monoclinic
space group	$P2(1)/n$	$P2(1)/c$
a, Å	12.464(1)	17.603(4)
b, Å	7.388(1)	6.827(2)
c, Å	12.702(1)	14.229(3)
β, deg	115.484(2)	113.281(3)
V, Å^3; Z	1055.9(2); 4	1570.6(6); 4
calcd density, Mg/m^3	1.591	1.758
abs coeff, mm^{-1}	1.070	2.285
F(000)	512	816
cryst size, mm	0.38 × 0.36 × 0.26	0.44 × 0.18 × 0.06
limiting indices	$-16 \le h \le 15$ $-9 \le k \le 9$ $-16 \le l \le 16$	$-23 \le h \le 21$ $-9 \le k \le 9$ $-19 \le l \le 19$
no. of reflns collected/ unique	12 420/2613	30 411/3898
abs corr	semiempirical for equiv	
refinement method	full-matrix least-squares of F^2	
no. of data/restraints/ params	2613/0/145	3898/0/184
GOF on F^2	1.062	1.094
final R indices ($I > 2\sigma(I)$)	$R_1 = 0.0245$ $wR_2 = 0.0683$	$R_1 = 0.0255$ $wR_2 = 0.0515$
R indices (all data)	$R_1 = 0.0254$ $wR_2 = 0.0691$	$R_1 = 0.0255$ $wR_2 = 0.0515$
largest diff peak and hole, e/Å^3	0.388 and −0.284	0.459 and −0.505

DFT Calculations. DFT calculations at the B3YP/6-31G* level were performed using Spartan (Wavefunction, Inc.). Tables of bond distances for **9**, **10**, and transition states **B** and **N** and charge densities of **9** are available in the Supporting Information.

Single-Crystal X-ray Crystallography. Crystals of **12** and **15** suitable for X-ray diffraction were obtained by recrystallization from CH_2Cl_2/hexanes and pentane, respectively. Crystallographic and data collection parameters are collected in Table 3. ORTEP drawings of **12** and **15** showing the atom-numbering schemes used in the refinements are given in Figures 1 and 2, respectively. Selected bond distances are collected in Table 2. Additional crystallographic data are available in the Supporting Information.

Acknowledgment. Partial support of this research has been provided by the National Science Foundation (Grant No. CHE-0108069.)

Supporting Information Available: CIF files giving X-ray characterization of **12** and **15**. Tables of calculated bond distances of **9**, **10**, **B**, and **N**. A table of calculated charge densities of **9.** This material is available free of charge via the Internet at http://pubs.acs.org.

OM060239+